Sushil Adhikari[1]
Sandun D. Fernando[2]
Agus Haryanto[3*]

[1] Department of Biosystems Engineering, Auburn University, Auburn, USA.

[2] Department of Biological and Agricultural Engineering, Texas A&M University, College Station, USA.

[3] Department of Agricultural and Biological Engineering, Mississippi State University, Mississippi State, USA.

Research Article

Kinetics and Reactor Modeling of Hydrogen Production from Glycerol via Steam Reforming Process over Ni/CeO_2 Catalysts

As a result of skyrocketing prices, environmental concerns and depletion associated with fossil fuels, renewable fuels are becoming attractive alternatives. In this respect, the demand for biodiesel has increased tremendously in recent years. Increased production of biodiesel has resulted in a glut of glycerol that has reduced the demand for this once valuable commodity. Consequently, finding alternative uses for glycerol is a timely proposition. One alternative is producing renewable hydrogen from this cheap commodity. Only a handful of studies have been conducted on producing hydrogen from glycerol. Previous studies have mainly focused on finding effective catalysts for glycerol steam reforming. This paper extends previous knowledge by presenting kinetic parameters in relation to glycerol steam reforming over Ni/CeO_2 and a reactor modeling. The study found that the activation energy and the reaction order for the glycerol steam reforming reaction over Ni/CeO_2 catalyst were 103.4 kJ/mol and 0.233, respectively.

Keywords: Biodiesel, Glycerol, Hydrogen, Nickel, Steam reforming

Received: September 12, 2008; *revised:* October 27, 2008; *accepted:* December 03, 2008

DOI: 10.1002/ceat.200800462

1 Introduction

In recent years, "hydrogen economy" has received much attention around the world. As a result, extensive research has been performed on finding sustainable sources for hydrogen. Biomass is an intriguing candidate for producing hydrogen. Our study focused on generating hydrogen from glycerol, a byproduct of biodiesel processing. In earlier studies, we tested several metal catalysts [1] and analyzed the effects of different supports [2] on hydrogen production from glycerol. The study found that CeO_2-supported Ni catalysts performed best compared to MgO- and TiO_2-supported catalysts in the steam reforming reaction. Other groups also studied hydrogen production from glycerol via steam reforming [3–5], autothermal [6, 7] and aqueous-phase reforming processes [8]. Most of these studies focused on catalyst performance testing. However, kinetics data were limited [9]. This study presents the kinetics of the glycerol steam reforming process and reactor modeling over a Ni-based CeO_2-supported catalyst. The overall reaction of the glycerol steam reforming process can be presented as in Eq. (1):

$$C_3H_8O_3 + 3\ H_2O \rightarrow 7\ H_2 + 3\ CO_2 \quad (1)$$

2 Methodology

2.1 Reaction Rate Expression

A power law model has previously been used to express the reaction kinetics for methanol [10] and ethanol [11, 12] steam reforming processes. Consequently, in this study, we used the power law model to fit experimental data. The model is in the form as given in Eq. (2):

$$r_a = k_0 \exp\left(-\frac{E}{RT}\right)[C_A]^n \quad (2)$$

where n represents the reaction order with respect to glycerol. E and T denote the activation energy and the reaction temperature, respectively. k_0 represents the reaction constant and R is the universal gas constant. The given form of the rate model does not include the water concentration because water was present in excess compared to the concentration of glycerol. It

Correspondence: Dr. Sandun D. Fernando (sfernando@tamu.edu), Department of Biological and Agricultural Engineering. Texas A & M University, College Station, TX 77843, USA.
*Present address: Agricultural Engineering Department, University of Lampung, Indonesia.

should be noted that a similar model was used for ethanol steam reforming in a previous work [12].

2.2 Kinetics Data

The experimental procedure outlined by Idem and Bakhshi [10] was followed to collect intrinsic kinetics data for the reaction. Mass transfer limitations were minimized by selecting an appropriate particle size range. Several catalyst particle size ranges were tested to determine whether the reaction was mass transfer limited. No changes in glycerol conversion were found with the increase in the particles from 60–70 to 80–100 U.S. sieve size. Consequently, particles of 60–80 range were used for the kinetics study. Film diffusion in the reaction system was also minimized by selecting suitable flow rates, and there was no significant change in glycerol conversion when the feed flow rate increased from 0.25 to 0.35 mL/min. Consequently, the feed flow rates that were used in our experiment ranged from 0.25 to 0.35 mL/min. The plug flow conditions in the reactor were also maintained by avoiding back mixing and to minimize channeling. The conditions to avoid back mixing and channeling are (i) ratio of the internal diameter of the tube to the catalyst particle size (d/D_p) >10 and (ii) ratio of the catalyst bed to the catalyst particle size (L/D_p) >50[13]. In this work, d/D_p and L/D_p were 49.1 and 142, respectively, and these values ensured plug flow conditions in the reactor. To maintain isothermal conditions in the reactor, the catalysts were mixed with inert materials (fused silica). The amount of inert materials was varied to maintain a pre-selected catalyst bed length. Intrinsic kinetics data for this study were collected at 873 and 923 K.

2.3 Catalyst Preparation

Nickel catalysts were prepared over a CeO_2 support (Nanoscale Materials, Manhattan, KS, USA). Catalysts were prepared by the incipient wetness technique using nickel nitrate hexahydrate [$Ni(NO_3)_2{\cdot}6\ H_2O$] purchased from Sigma-Aldrich (St. Louis, MO, USA). Catalysts were dried at 383 K for 12 h and calcined at 773 K for 6 h in air. The furnace temperatures were ramped at 10 K/min for catalyst drying and calcination. After drying, the catalyst samples were sieved for an appropriate size and selected size ranges were used for analysis.

2.4 Catalyst Performance Testing

All experiments were carried out in a tubular furnace that could reach temperatures up to 1373 K. Glycerol and water were mixed in a separate container at pre-selected molar ratios prior to the experiments. The mixture was then introduced into the tubular reactor using a high-pressure liquid chromatography (HPLC) pump (LC-20AT; Shimadzu Scientific Instrument, Columbia, MD, USA). Catalysts were diluted with fused silica of similar size to maintain an isothermal condition, and the mixture of catalyst and fused silica was placed inside a reactor using quartz wool. The reactor was made of quartz with 0.5 inch outer diameter and 0.054 inch wall thickness and was purchased from Technical Glass Products (Painesville Twp., OH, USA). Prior to the experiment, the catalysts were reduced by sending H_2 gas (50 mL/min) for 1 h at 973 K.

The output gas stream from the reactor was cooled using crushed ice and water. Unreacted water, glycerol, and other liquids that formed during the reaction were collected at room temperature by condensing. The condensate was used to analyze glycerol conversion. Fig. 1 illustrates the glycerol steam reforming process schematically. Hydrogen gas (Fig. 1) was used only during the catalyst reduction process. An HPLC system (1200; Agilent Technologies Inc., Palo Alto, CA, USA) was used to analyze glycerol conversion with a Zorbax carbohydrate column (4.6 × 150 mm, 5 μm) using a mixture of acetonitrile and water as the mobile phase. Outlet gases were passed through a moisture trap before sending into a gas chromatograph unit (GC6890; Agilent Technologies Inc.). The hydrogen content in the gas mixture was analyzed by a thermal conductivity detector with an HP-Plot molecular sieve column. Concentrations of carbon monoxide (CO), methane (CH_4), carbon dioxide (CO_2), ethane (C_2H_6), and ethylene (C_2H_4) were analyzed by a flame ionization detector with an

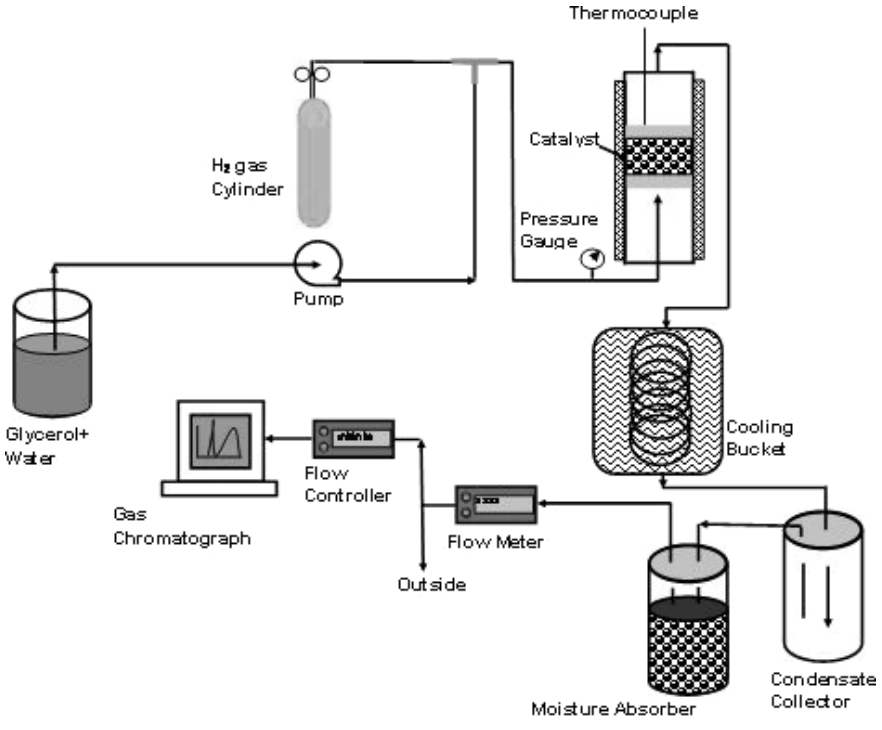

Figure 1. Schematic of the glycerol steam reforming system.

HP-Plot Q column. Altogether, six gases including H_2 were analyzed.

2.5 Numerical Modeling

The numerical model for a packed-bed tubular reactor was developed based on the steady-state mass and energy balance. The model was based on the following assumptions: (i) pseudo-homogeneous chemical phase, (ii) constant density, (iii) constant velocity, (iv) constant wall temperature, (v) negligible pressure drop, (vi) gas ideal law. The mathematical model could be presented in the cylindrical coordinates, and the mass and energy balance for species i can be written as follows [14, 15]:

$$D_r\left[\frac{\partial^2 C_i}{\partial r^2}+\frac{1}{r}\frac{\partial C_i}{\partial r}\right]+D_z\frac{\partial^2 C_i}{\partial z^2}+\rho_b r_i=v\frac{\partial C_i}{\partial z} \tag{3}$$

$$\lambda_r\left[\frac{\partial^2 T}{\partial r^2}+\frac{1}{r}\frac{\partial T}{\partial r}\right]+\lambda_z\frac{\partial^2 T}{\partial z^2}+\rho_b\left[\sum -\Delta H r_i\right]=v\rho_g C_p\frac{\partial T}{\partial z} \tag{4}$$

where D_z and D_r denote the effective diffusivity in axial and radial directions, respectively. λ_r and λ_z denote the radial and axial effective thermal conductivity, respectively. v denotes velocity in the axial direction, C_i is the concentration of species i, ρ_b denotes the catalyst bed density, ρ_g denotes the gas density, C_p denotes the heat capacity, r_i denotes the reaction rate for species i, T denotes the temperature, and ΔH denotes the heat of reaction.

The initial and boundary conditions for the steady-state energy and mass balance equations were as follows:

$$C_i(r,0)=C_i^0, T(r,0)=T_i^0, \text{at } z=0 \text{ and } 0\le r\le r_{id} \tag{5}$$

$$\frac{\partial C_i}{\partial r}(0,z)=0\frac{\partial T}{\partial r}(0,z)=0 \text{ at } r=0 \text{ and } 0\le z\le L \tag{6}$$

$$\frac{\partial C_i}{\partial r}(r_{id},z)=0, \lambda_r\frac{\partial T}{\partial r}(r_{id},z)=U_{TW}(T_1-T_2), \text{ at } r=r_{id} \text{ and } 0\le z\le L \tag{7}$$

where U_{TW} denotes the overall heat transfer coefficient of the tube and the superscript 0 denotes the inlet condition.

3 Results and Discussion

3.1 Activation Energy and Reaction Order

Glycerol conversion in this study was defined as given below:

$$X=\frac{\text{Glycerol in}-\text{Glycerol out}}{\text{Glycerol in}} \tag{8}$$

A design equation for the plug flow reactor was used for data analysis and the rate expression was expressed in the differential form as shown below [12]:

$$r_a=\frac{dX}{d\left(\frac{W}{F_{A0}}\right)} \tag{9}$$

where W and F_{A0} denote weight of the catalyst and feed flow rate, respectively.

To obtain the experimental reaction rates, slopes were taken as various points of X vs. W/F_{A0} curves within the range of the operation conditions. Tab. 1 shows the kinetics data and the experimental reaction rates as described in Eq. (9). The equilibrium constant (K_p) was calculated as given in Eq. (10):

$$\ln K_p=-\frac{\Delta G}{RT} \tag{10}$$

where ΔG is the Gibbs energy change of reaction, R is the universal gas constant and T is the absolute temperature of reaction.

The values of activation energy and reaction order based on the power model (Eq. (2)) were estimated with nonlinear regression analysis using the Marquardt algorithm using SAS 9.1 software [16]. The activation energy and the reaction order were found to be 103.4 kJ/mol and 0.233, respectively. The reaction constant was found to be 8135.5 $kmol^{0.767}/(s^{0.767}$ kgcat). Simonetti et al. [9] had reported activation energies of 60–90 kJ/mol for Pt and Pt-Re catalysts and the reaction order of 0.2 for glycerol. The activation energy is slightly higher and the reaction order is close to the findings of Simonetti et al. [9]. Fig. 2 depicts the comparison of measured and predicted rates using Eq. (8). Some data points were not fitted well and it appears that the data represent two regimes. However, when the data obtained at 823 K were tried to fit in Eq. (2), the model did not converge. This might be because of a few data points. However, if all the data (at 873 and 923 K) were used to fit in Eq. (2), the model did converge. Because of the simplicity of the rate expression and because the results were close to the published data, the model and the values for activation energy and reaction order have been accepted.

3.2 Model Prediction

Reactor modeling was performed using COMSOL® software. Tab. 2 gives the parameters and their values used for predicting the model. The data for gas density and the overall heat transfer coefficient were taken from Akande et al. [12]. The data for heat capacity and effective thermal conductivity were taken from Akpan et al. [17]. The data for effective diffusivity was calculated using the Gilliland equation [18].

Fig. 3 illustrates the comparison between experimental glycerol conversion and model-predicted conversion predicted using COMSOL®. The average deviation between the experimental values and the model prediction was about 6.7 %.

Table 1. Experimental reaction rates and intrinsic kinetics data for glycerol steam reforming.

Run	Rate of reaction [$kmol_{glycerol}/kg_{cat}$ s]	C_A [kmol/s]	C_B [kmol/s]	C_C [kmol/s]	C_D [kmol/s]	K_p
1	5.56E–05	5.341E–09	1.632E–07	3.941E–09	2.474E–08	1.17E+25
2	6.50E–05	5.907E–09	1.638E–07	1.365E–10	7.763E–09	1.17E+25
3	6.04E–05	5.582E–09	1.635E–07	2.795E–09	2.008E–08	1.17E+25
4	5.06E–05	5.054E–09	1.630E–07	3.057E–09	2.162E–08	1.17E+25
5	4.57E–05	4.813E–09	1.627E–07	3.501E–09	2.346E–08	1.17E+25
6	8.13E–05	1.144E–09	1.590E–07	3.046E–09	1.412E–08	4.07E+25
7	6.70E–05	4.163E–10	1.583E–07	5.224E–09	1.913E–08	4.07E+25
8	7.50E–05	7.077E–10	1.586E–07	5.052E–09	2.056E–08	4.07E+25
9	9.32E–05	1.980E–09	1.599E–07	3.896E–09	1.492E–08	4.07E+25
10	1.01E–04	2.422E–09	1.603E–07	3.106E–09	1.681E–08	4.07E+25

A = $C_3H_8O_3$; B = H_2O; C = CO_2; D = H_2; K_p = equilibrium constant.

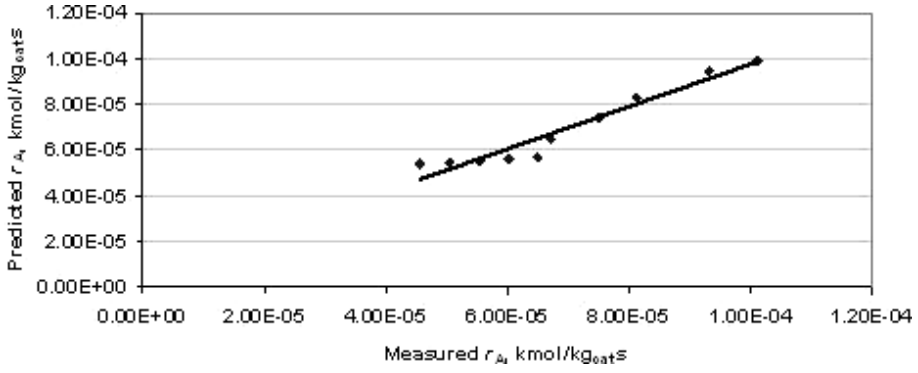

Figure 2. Comparison of the experimental reaction and the predicted rates using the rate model.

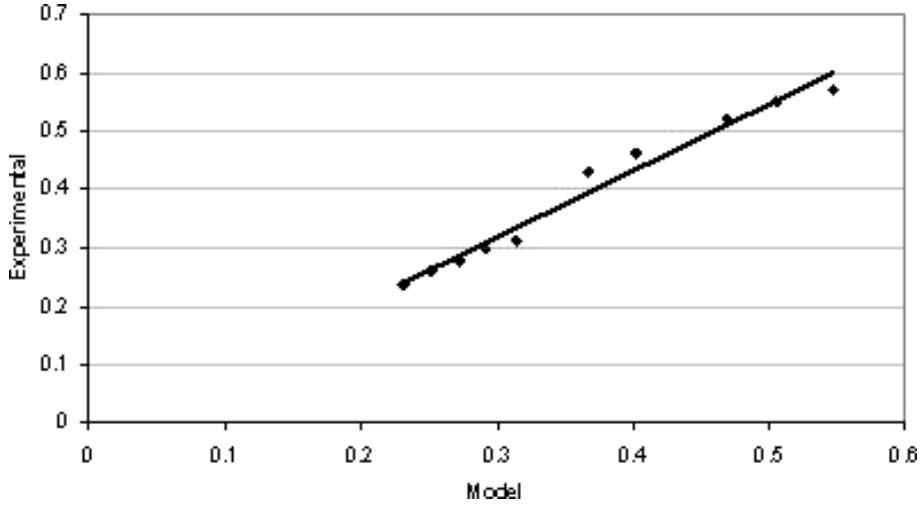

Figure 3. Comparison between experimental and model-predicted glycerol conversion.

Table 2. Parameters and values used in the reactor modeling.

Parameter	Definition	Values and units
T_0	Temperature	873 K
v	Superficial velocity	$51.5 \cdot 10^{-3}$ m/s
ρ_b	Bulk density	20.55 kg/m^3
ρ_g	Gas density	0.31 kg/m^3
D_z and D_r	Effective diffusivity	$7.57 \cdot 10^{-9}$ m^2/s
U_{TW}	Heat transfer coefficient	0.156 kW/m^2 K
E	Activation energy	103.4 kJ/mol
k	Rate constant	8135.5
λ_z and λ_r	Effective thermal conductivity	$9.37 \cdot 10^{-3}$ kW/m K
C_p	Heat capacity	2.07 kJ/kg K
ε	Void fraction	0.22
y_{A0}	Inlet mole fraction of glycerol	0.076
M	Molecular weight	92.09 g/mol
r	Internal radius of the reactor	5.08 mm
L	Length of the reactor	30 mm

Fig. 4 presents the effect of reaction temperature on glycerol conversion. As can be seen, glycerol conversion increased with the increase in temperature. Similarly, Fig. 5 depicts the effect of catalyst amount in a reaction bed (or bed density). As expected, glycerol conversion increased with the increase in catalyst amount. Fig. 6 depicts the reduction in temperature along the catalyst bed. The temperature was reduced by about 3.5 K during the reaction, and this was mainly due to the endothermic nature of the reaction.

4 Conclusions

The activation energy and the reaction order for the glycerol steam reforming reaction over Ni/CeO_2 catalyst were found to be 103.4 kJ/mol and 0.233, respectively, based on a power model. A mathematical model was developed to determine the glycerol conversion, and the average deviation was 6.7% between the experimental conversion and the model-predicted values.

Symbols used

C_p	[kJ/kg K]	Heat capacity
D_z, D_r	[m^2/s]	Effective diffusivity
E	[kJ/mol]	Activation energy
k	[–]	Rate constant
L	[mm]	Length of the reactor
M	[g/mol]	Molecular weight
r	[mm]	Internal radius of the reactor

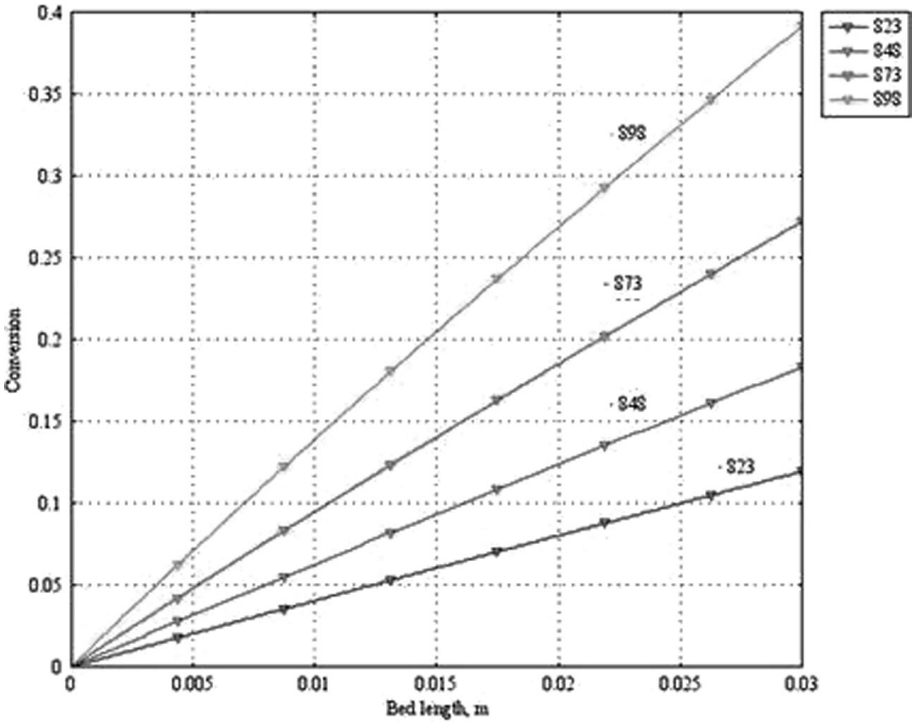

Figure 4. Effect of glycerol conversion along the bed at various reaction temperatures (in K) at a bed density of 24.69 kg/m^3.

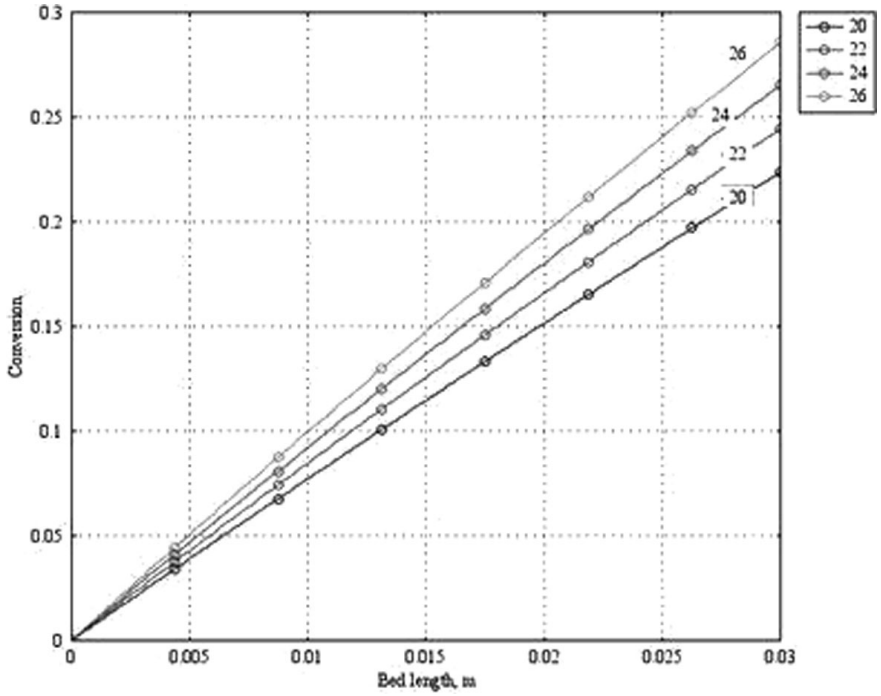

Figure 5. Effect of glycerol conversion along the bed at various bed densities (in kg/m^3) at 873 K.

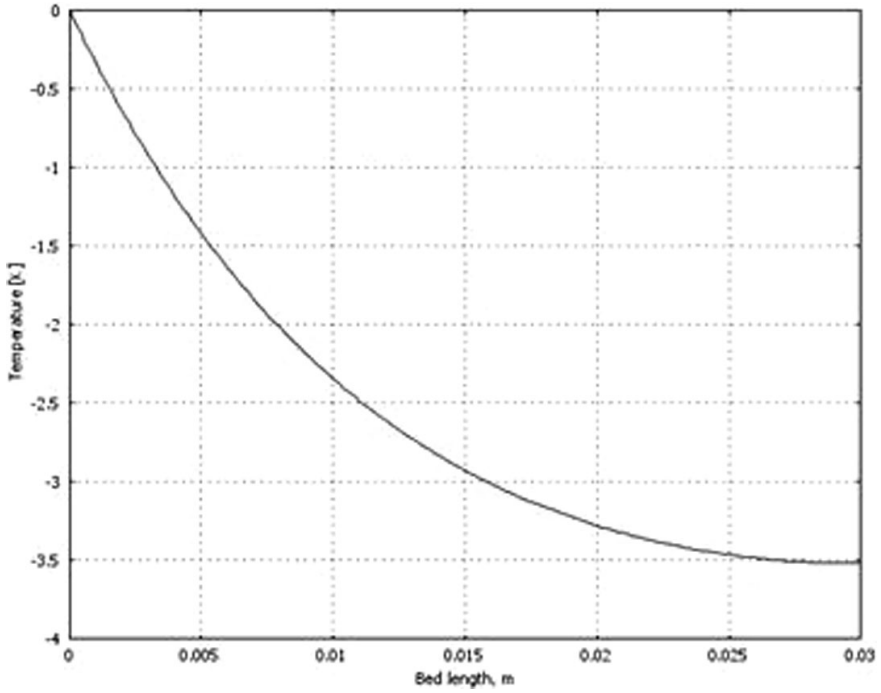

Figure 6. Change in temperature along the catalyst bed at 873 K and a bed density of 24.69 kg/m^3.

T_0	[K]	Temperature
U_{TW}	[kW/m^2 K]	Heat transfer coefficient
v	[m/s]	Superficial velocity
y_{A0}	[–]	Inlet mole fraction of glycerol

Greek letters

ε	[–]	Void fraction
λ_z, λ_r	[kW/m K]	Effective thermal conductivity
ρ_b	[kg/m^3]	Bulk density
ρ_g	[kg/m^3]	Gas density

References

[1] S. Adhikari, S. Fernando, A. Haryanto, *Catal Today* **2007**, *129*, 355.
[2] S. Adhikari, S. Fernando, S. D. F. To, R. M. Bricka, P. H. Steele, A. Haryanto, *Energy Fuels* **2008**, *22*, 1220.
[3] B. Zhang, X. Tang, Y. Li, Y. Xu, W. Shen, *Int. J. Hydrogen Energy* **2007**, *32*, 2367.
[4] T. Hirai, N.-O. Ikenaga, T. Mayake, T. Suzuki, *Energy Fuels* **2005**, *19*, 1761.
[5] S. Czernik, R. French, C. Feik, E. Chornet, *Ind. Eng. Chem. Res.* **2002**, *41*, 4209.
[6] P. J. Dauenhauer, J. R. Salge, L. D. Schmidt, *J. Catal.* **2006**, *244*, 238.
[7] S. M. Swami, M. A. Abraham, *Energy Fuels* **2006**, *20*, 2616.
[8] R. D. Cortright, R. R. Davda, J. A. Dumesic, *Nature* **2002**, *418*, 964.
[9] D. A. Simonetti, E. L. Kunkes, J. A. Dumesic, *J. Catal.* **2007**, *247*, 298.
[10] R. O. Idem, N. N. Bakhshi, *Chem. Eng. Sci.* **1996**, *51*, 3697.
[11] D. A. Morgenstern, J. P. Fornango, *Energy Fuels* **2005**, *19*, 1708.
[12] A. Akande, A. Aboudheir, R. Idem, A. Dalai, *Int. J. Hydrogen Energy* **2006**, *31*, 1707.
[13] H. F. Rase, *Chemical Reactor Design for Process Plants: Principles and Techniques*, John Wiley & Sons, New York **1977**, 185.
[14] R. B. Bird, W. E. Stewart, E. N. Lightfoot, *Transport Phenomena*, 2nd ed., John Wiley & Sons, Inc., New York **2002**.
[15] A. Aboudheir, A. Akande, R. Idem, A. Dalai, *Int. J. Hydrogen Energy* **2006**, *31*, 752.
[16] SAS Institute Inc., *Statistical Analysis Software*, Cary **2003**.
[17] E. Akpan, A. Akande, A. Aboudheir, H. Ibrahim, R. Idem, *Chem. Eng. Sci.* **2007**, *62*, 3112.
[18] R. H. Perry, D. W. Green, J. O. Maloney, *Perry's Chemical Engineer's Handbook*, 7th ed., McGraw-Hill, New York **1997**.

DOI: 10.1002/ceat.200800462

Research Article: This paper presents kinetic parameters in relation to glycerol steam reforming over Ni/CeO_2 and a reactor modeling. The study found that the activation energy and the reaction order for the glycerol steam reforming reaction over Ni/CeO_2 catalyst were 103.4 kJ/mol and 0.233, respectively.

Kinetics and Reactor Modeling of Hydrogen Production from Glycerol via Steam Reforming Process over Ni/CeO_2 Catalysts

S. Adhikari, S. D. Fernando*, and A. Haryanto

Chem. Eng. Technol. **2009**, *32 (4)*, XXX ... XXX